

Plasmons in finite spherical ionic systems

W. Jacak

*Institute of Physics, Wrocław University of Technology,
Wyb. Wyspiańskiego 27, 50-370 Wrocław, Poland,*

(Dated: Received: date / Accepted: date)

The challenging question on possible plasmon type excitations in finite ionic systems is discussed. Related theoretical model is formulated and developed in order to describe surface and volume plasmons of ion liquid in finite electrolyte systems. Irradiation of ionic surface plasmon fluctuations is studied in terms of the Lorentz friction of oscillating charges. Attenuation of surface plasmons in the ionic sphere is calculated and minimized with respect to the sphere size. Various regimes of approximation for description of size effect for damping of ionic plasmons are determined and a cross-over in damping size-dependence is demonstrated. The most convenient, optimal dimension of finite electrolyte system for energy and information transfer by usage of ionic dipole plasmons is determined. The overall shift of size effect to micrometer scale for ions in comparison to nanometer scale for electrons in metals is found, as well as the red shift by several orders of plasmonic resonances in ion systems predicted in a wide range of variation depending on ion system parameters. This convenient opportunity of tuning resonances differs properties of ionic plasmons from plasmons in metals where electron concentration is firmly fixed.

I. INTRODUCTION

Recent experimental and theoretical investigation of plasmon oscillations in metallic nanoparticles focused attention on the fundamental character of this phenomenon and also on great prospects of applications. In particular, the so-called plasmon effect in solar cells modified in nano-scale with on surface deposited metallic particles leads to the significant growth of their efficiency [1–6]. The mediating role in collecting of sun-light energy is played by surface plasmon oscillations in metallic nanoparticles due to their radiative properties. Irradiation of energy of plasmon oscillations is preferable for energy transport applications. As it was observed experimentally and later predicted theoretically, irradiation losses of plasmon energy are strongly sensitive to the metallic nanoparticles size [7].

Strong irradiation of plasmon oscillations in metallic nanoparticles plays also a major role in construction of plasmonic wave-guides with high transference efficiency. Many experimental studies [8, 9] indicated that periodic linear structures of metallic nanoparticles serve as efficient plasmon wave-guides with low damping [10–12]. The wave-lengths of propagating in such structures plasmon-polaritons typically are by one order shorter in comparison to light with the same frequency, which allows for avoiding diffraction limits in optical circuits [13–15]. This is perceived as a way to forthcoming constructions of plasmon opto-electronic nano-devices, not attainable by using only light wave-guides limited by diffraction constraints. An efficient energy transfer in plasmon wave-guides is also conditioned by radiative properties of surface plasmons in metallic nano-components.

Radiative losses of plasmon oscillations can be described by the so-called Lorentz friction [16, 17]. Accelerating charges irradiate electro-magnetic wave and the related energy loss can be accounted for as an effective electric field which hampers electron movement. For the case of the oscillating dipole as for the dipole-type surface plasmons in a metallic nanosphere, the Lorentz friction force is proportional to the third order time-derivative of this dipole [16]. Let us emphasize here that the strong irradiation of surface plasmons in metallic nanospheres, linked to the Lorentz friction, is exclusively present in sufficiently large metallic nano-particles. Small metallic nano-particles in form of the clusters of size 1 – 5 nm do not exhibit irradiation efficiency so high as nanospheres with radii $a > 10$ nm. Especially much attention was focused on large nanoparticles of noble metals (gold, silver and copper) because of location of plasmon resonances in particles of these metals within the visible light spectrum.

An interesting question which we try to discuss in the present paper is the possibility for occurrence of similar plasmon effects with ionic carriers instead of electrons. Many finite ionic systems in a form of enclosed by membranes electrolyte systems can be encountered in biological structures and the question arises regarding possible significance of such ion plasmonic phenomena, the role it would take in such structures and whether the radiative properties of plasmon fluctuation would also be so pronounced in ionic system as they were in metals. It is quite reasonable that ionic plasmon effect would be located in other regions of energy and wave lengths in comparison to metallic systems. This, let's call it 'soft' plasmonics could be linked with functionality of biological systems where electricity is rather of ionic than electronic character. For instance the cell signaling, membrane transfer or nerve cell conductivity would serve as examples.

The theoretical plasmonic model we will adopt for ions, as far as possible, upon analogy to the metallic nanospheres with plasmon excitations theory. The ionic systems are much more complicated in comparison to a metal crystal structure with free electrons. Therefore, an identification of an appropriate simplifications of the approach to ionic system is of a primary significance. The model must be capable of repetition for ions in electrolyte the plasmonic scenario known from electrons in metals.

In the present paper we will consider the finite spherical ionic system (e.g., liquid electrolyte artificially confined with a membrane) and identify the plasmon excitations of ions in this system. We will determine their energies for various parameters of the ionic system with special attention paid to irradiation properties of ionic plasmons.

In the subsequent paper [18] we will analyze an ionic plasmon-polariton propagation in electrolyte sphere chains with prospective relation to signaling in biological systems. Taking in mind that metallic nano-chains serve as very efficient wave-guides for electro-magnetic signals in the form of collective surface plasmon excitation of wave-type called plasmon-polaritons, we will try to model the similar phenomenon in the ionic spheres chains.

For the initial crude model we will study the spherical or prolate spheroidal ionic conducting system with balanced charges in analogy to the jellium model in metals when local fluctuations of ion density, negative and positive beyond the equilibrium level, can form plasmons in ionic finite system [19].

II. FLUCTUATIONS OF THE CHARGE DENSITY IN THE SINGLE CONDUCTING IONIC SPHERICAL SYSTEM

The problem of how to establish an adequate model for multi-ionic system to grasp essential properties of ionic plasmons is a main issue. For simple two-component ionic system we deal with both sign ion solutions creating an electrolyte with balanced negative and positive total charge. In equilibrium these charge cancellation is also local. As

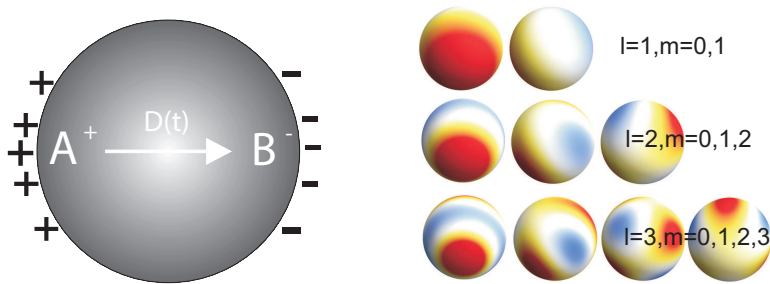


FIG. 1. Dipole $\mathbf{D}(\mathbf{t})$ creation in a single sphere by the simplest surface plasmon oscillations (left); examples of surface plasmon charge distribution with various multiplicity l , m —different colors indicate distinct values of local charge density from negative to positive ones (right)

we deal with two kinds of carriers they both would form density fluctuations resulting in violation of the local electric equilibrium. The total compensation of both sign charges requires, however, that any density fluctuation of negative charges must be accompanied by distant, in general, but ideally equivalent positive ions fluctuation, and conversely. This means that effectively we deal with density fluctuation of ions, either positive or negative in charge value (always mutually compensated) with respect to uniform charge distribution assumed as ideally cancelled by the opposite sign uniform background—fictitious jellium in analogy to metal. In this way we can model a two component ionic system by two single component ion systems with jellium of the opposite sign. For simplicity we assume that the charge and mass of the opposite ions are the same, but generalization is straightforward.

To simplify the model according to the above described lines let us consider the spherical shape system with the radius a and with balanced total charge of both sign ions with uniform equilibrium density distributions $n^{+(-)}(\mathbf{r}) = n\Theta(a - r)$ ($\Theta(r)$ is the Heaviside step function, a is the sphere radius). For simplicity, we assume the same absolute value of charges of plus- and minus-charged ions. By $m^{+(-)}$ one can denote the mass of positive (negative) ions. They both are of the order of $10^{4-5}m_e$, where $m_e = 3.1 \times 10^{-31}$ kg, is the mass of the electron. Reducing the two component system to two systems with the jellium, is an approximation but may serve for a recognition of ionic dynamics and of scales for its quantitative characteristics, at least. The advantage of such an approach is a close analogy to description of plasmon in metals including direct definition of the rigid shape of the system by the explicit jellium form.

Upon the above model assumptions we will consider the ionic carries with density oscillating around the zero valued equilibrium density as screened by the fictitious positive charged background (the effect of the opposite sign ions presence). Hence, the description of fluctuations of local density of electrons in metallic nanosphere can be directly used to model fluctuations of effective ions density, substituting electron mass by the ion mass and the electron charge by the ion charge. The dynamical equation for the charged fluid in ion system can be thus repeated from the case of metal nanosphere with electrons [19]. The equilibrium density of the effective charged liquid, denoted by n , will be treated as a parameter and assumed equal to $n = \eta N_0$ where η is the molarity of the electrolyte in the sphere and N_0 is the one-molar electrolyte concentration of ions. The equilibrium density determines the bulk plasmon frequency for the ion system according to the formula, $\omega_p^2 = \frac{4\pi n q^2}{m}$, where n and m are the equilibrium uniform concentration and the mass of ions with the charge q . Due to larger m than the electron mass, m_e , and usually smaller concentration of effective ions than the one for electrons in metals, ω_p can be considerably reduced, even by several orders of magnitude. Note, that for electrons in metals $\hbar\omega_p \simeq 10$ eV and typically falls into ultra-violet region of radiation with corresponding energy of photons. In the ionic system, the plasmon frequency $\hbar\omega_p$ can be much lower and placed in the range of infra-red or even in lower energy part of the electro-magnetic wave spectrum.

A. Definition of the model

The Hamiltonian for the two type ion system has the form,

$$\hat{H}_{ion} = -\sum_{i=1}^{N^-} \frac{\hbar^2 \nabla_i^2}{2m^-} - \sum_{j=1}^{N^+} \frac{\hbar^2 \nabla_j^2}{2m^+} - \sum_{i,j}^{N^-, N^+} \frac{q^- q^+}{\varepsilon |\mathbf{r}_i - \mathbf{r}_j|} + \frac{1}{2} \sum_{i,i',i \neq i'}^{N^-} \frac{(q^-)^2}{\varepsilon |\mathbf{r}_i - \mathbf{r}_{i'}|} + \frac{1}{2} \sum_{j,j',j \neq j'}^{N^+} \frac{(q^+)^2}{\varepsilon |\mathbf{r}_j - \mathbf{r}_{j'}|}, \quad (1)$$

where $q^{-(+)}$, $M^{-(+)}$, $N^{-(+)}$ are the charge, the mass and the number of the $-(+)$ ions, respectively. To analyze this complicated system we propose the following approximation, assuming, for simplicity, $q^- = -q^+ = q$, $N^- = N^+ = N$,

$m^- = m^+ = m$ and let us add and subtract the same terms as written below,

$$\begin{aligned} \hat{H}_{ion} = & - \sum_{i=1}^N \frac{\hbar^2 \nabla_i^2}{2m} - \sum_{j=1}^N \frac{\hbar^2 \nabla_j^2}{2m} - \sum_{i,j} \frac{q^2}{\varepsilon |\mathbf{r}_i - \mathbf{r}_j|} + \frac{1}{2} \sum_{i,i',i \neq i'} \frac{q^2}{\varepsilon |\mathbf{r}_i - \mathbf{r}_{i'}|} + \frac{1}{2} \sum_{j,j',j \neq j'} \frac{q^2}{\varepsilon |\mathbf{r}_j - \mathbf{r}_{j'}|} \\ & - q^2 \sum_j \int \frac{n(\mathbf{r}) d^3 \mathbf{r}}{\varepsilon |\mathbf{r}_j - \mathbf{r}|} - q^2 \sum_i \int \frac{n(\mathbf{r}) d^3 \mathbf{r}}{\varepsilon |\mathbf{r}_i - \mathbf{r}|} + q^2 \sum_j \int \frac{n(\mathbf{r}) d^3 \mathbf{r}}{\varepsilon |\mathbf{r}_j - \mathbf{r}|} + q^2 \sum_i \int \frac{n(\mathbf{r}) d^3 \mathbf{r}}{\varepsilon |\mathbf{r}_i - \mathbf{r}|}, \end{aligned} \quad (2)$$

where we have introduced formally the jellium of the spherical shape for both types of ions, with the density n ideally compensating opposite charges of uniformly distributed ions, $n(\mathbf{r}) = n\Theta(a - r)$, a is the sphere radius (the positive jellium with the negative jellium mutually cancel themselves). Assuming that $q^2 \sum_j \int \frac{n(\mathbf{r}) d^3 \mathbf{r}}{\varepsilon |\mathbf{r}_j - \mathbf{r}|} + q^2 \sum_i \int \frac{n(\mathbf{r}) d^3 \mathbf{r}}{\varepsilon |\mathbf{r}_i - \mathbf{r}|} - \sum_{i,j} \frac{q^2}{\varepsilon |\mathbf{r}_i - \mathbf{r}_j|} \simeq 0$, which is fulfilled for not too strong ion concentration fluctuations beyond the uniform distribution,

we can separate the Hamiltonian into the sum, $\hat{H}_{ions} = \hat{H}^- + \hat{H}^+$, where,

$$\hat{H}^{-(+)} = \sum_j \left[-\frac{\hbar^2 \nabla_j^2}{2m} - q^2 \int \frac{n(\mathbf{r}) d^3 \mathbf{r}}{\varepsilon |\mathbf{r}_j - \mathbf{r}|} \right] + \frac{1}{2} \sum_{j \neq j'} \frac{q^2}{\varepsilon |\mathbf{r}_j - \mathbf{r}_{j'}|}. \quad (3)$$

The latter term in r.h.s. of Eq. (3) corresponds to interaction between ions of the same sign, whereas the second term in the first sum describes interaction of these ions with the effective jellium (of opposite sign), ε is the dielectric constant of the electrolyte medium. The confined electrolyte system could be, in particular, a electrolyte medium shaped by appropriately formed membrane, as frequently occurs in biological systems. Because of separation of the Hamiltonian (1) one can consider single Hamiltonian (3). The ion wave function corresponding to Hamiltonian (3) is denoted by $\Psi_{ion}(t)$.

The form of Hamiltonian (3) allows for repetition of its further discussing along the scheme applied to electrons in metals [19], which we will recall below, for the sake of completeness. A local density of chosen type ions can be written, in analogy to semiclassical Pines-Bhom random phase approximation (RPA) approach to electrons in metal [20, 21], in the following form:

$$\rho(\mathbf{r}, t) = \langle \Psi_{ion}(t) | \sum_j \delta(\mathbf{r} - \mathbf{r}_j) | \Psi_{ion}(t) \rangle, \quad (4)$$

where \mathbf{r}_j denotes coordinate of j -th ion and the Dirac delta quasiclassically fixes j -th ion position. The Fourier picture of the above density has the form:

$$\tilde{\rho}(\mathbf{k}, t) = \int \rho(\mathbf{r}, t) e^{-i\mathbf{k} \cdot \mathbf{r}} d^3 r = \langle \Psi_{ion}(t) | \hat{\rho}(\mathbf{k}) | \Psi_{ion}(t) \rangle, \quad (5)$$

where the 'operator' $\hat{\rho}(\mathbf{k}) = \sum_j e^{-i\mathbf{k} \cdot \mathbf{r}_j}$.

Using the above notation one can rewrite \hat{H}_{ion} in the following form, in an analogy to the bulk case for metallic plasmon description [19–21]:

$$\hat{H}_{ion} = \sum_{j=1}^N \left[-\frac{\hbar^2 \nabla_j^2}{2m} \right] - \frac{q'^2}{(2\pi)^3} \int d^3 k \tilde{n}(\mathbf{k}) \frac{2\pi}{k^2} \left(\hat{\rho}^+(\mathbf{k}) + \hat{\rho}(\mathbf{k}) \right) + \frac{q'^2}{(2\pi)^3} \int d^3 k \frac{2\pi}{k^2} \left[\hat{\rho}^+(\mathbf{k}) \hat{\rho}(\mathbf{k}) - N \right], \quad (6)$$

where: $\tilde{n}(\mathbf{k}) = \int d^3 r n(\mathbf{r}) e^{-i\mathbf{k} \cdot \mathbf{r}}$ is the Fourier picture of jellium distribution (in the derivation of Eq. (6) we have taken into account that $\frac{4\pi}{k^2} = \int d^3 r \frac{1}{r} e^{-i\mathbf{k} \cdot \mathbf{r}}$, $q'^2 = \frac{q^2}{\varepsilon}$).

Utilizing this form of the effective ion Hamiltonian one can write out the dynamic equation in Heisenberg representation for ion density fluctuations,

$$\frac{d^2 \hat{\rho}(\mathbf{k})}{dt^2} = \frac{1}{(i\hbar)^2} \left[\left[\hat{\rho}(\mathbf{k}), \hat{H}_{ion} \right], \hat{H}_{ion} \right], \quad (7)$$

which attains the following form,

$$\begin{aligned} \frac{d^2 \hat{\rho}(\mathbf{k})}{dt^2} = & - \sum_j e^{-i\mathbf{k} \cdot \mathbf{r}_j} \left\{ -\frac{\hbar^2}{m^2} (\mathbf{k} \cdot \nabla_j)^2 + \frac{\hbar^2 k^2}{m^2} i\mathbf{k} \cdot \nabla_j + \frac{\hbar^2 k^4}{4m^2} \right\} \\ & - \frac{4\pi q'^2}{m(2\pi)^3} \int d^3 p \tilde{n}(\mathbf{p}) \frac{\mathbf{k} \cdot \mathbf{p}}{p^2} \hat{\rho}(\mathbf{k} - \mathbf{p}) - \frac{4\pi q'^2}{m(2\pi)^3} \int d^3 p \hat{\rho}(\mathbf{k} - \mathbf{p}) \frac{\mathbf{k} \cdot \mathbf{p}}{p^2} \hat{\rho}(\mathbf{p}). \end{aligned} \quad (8)$$

One can notice that $\hat{\rho}(\mathbf{k}-\mathbf{p})\hat{\rho}(\mathbf{p}) = \delta\hat{\rho}(\mathbf{k}-\mathbf{p})\delta\hat{\rho}(\mathbf{p}) + \tilde{n}(\mathbf{k}-\mathbf{p})\delta\hat{\rho}(\mathbf{p}) + \delta\hat{\rho}(\mathbf{k}-\mathbf{p})\tilde{n}(\mathbf{p}) + \tilde{n}(\mathbf{k}-\mathbf{p})\tilde{n}(\mathbf{p})$ and $\tilde{n}(\mathbf{p})\hat{\rho}(\mathbf{k}-\mathbf{p}) = \tilde{n}(\mathbf{p})\delta\hat{\rho}(\mathbf{k}-\mathbf{p}) + \tilde{n}(\mathbf{p})\tilde{n}(\mathbf{k}-\mathbf{p})$, where $\delta\hat{\rho}(\mathbf{k}) = \hat{\rho}(\mathbf{k}) - \tilde{n}(\mathbf{k})$ describes the 'operator' of local ion density fluctuation above the uniform distribution. Therefore, one can rewrite Eq. (8) as follows,

$$\begin{aligned} \frac{d^2\delta\hat{\rho}(\mathbf{k})}{dt^2} &= -\sum_j e^{-i\mathbf{k}\cdot\mathbf{r}_j} \left\{ -\frac{\hbar^2}{m^2} (\mathbf{k}\cdot\nabla_j)^2 + \frac{\hbar^2 k^2}{m^2} i\mathbf{k}\cdot\nabla_j + \frac{\hbar^2 k^4}{4m^2} \right\} \\ &- \frac{4\pi q'^2}{m(2\pi)^3} \int d^3p \tilde{n}(\mathbf{k}-\mathbf{p}) \frac{\mathbf{k}\cdot\mathbf{p}}{p^2} \delta\hat{\rho}(\mathbf{p}) - \frac{4\pi q'^2}{m(2\pi)^3} \int d^3p \delta\hat{\rho}(\mathbf{k}-\mathbf{p}) \frac{\mathbf{k}\cdot\mathbf{p}}{p^2} \delta\hat{\rho}(\mathbf{p}). \end{aligned} \quad (9)$$

Taking averaging over the quantum states $|\Psi_{ion}\rangle$, for the ion density fluctuation $\delta\tilde{\rho}(\mathbf{k}, t) = \langle \Psi_{ion} | \delta\hat{\rho}(\mathbf{k}, t) | \Psi_{ion} \rangle = \tilde{\rho}(\mathbf{k}, t) - \tilde{n}(\mathbf{k})$, we obtain the following equation,

$$\begin{aligned} \frac{\partial^2\delta\tilde{\rho}(\mathbf{k}, t)}{\partial t^2} &= -\langle \Psi_{ion} | \sum_j e^{-i\mathbf{k}\cdot\mathbf{r}_j} \left\{ -\frac{\hbar^2}{m^2} (\mathbf{k}\cdot\nabla_j)^2 + \frac{\hbar^2 k^2}{m^2} i\mathbf{k}\cdot\nabla_j + \frac{\hbar^2 k^4}{4m^2} \right\} | \Psi_{ion} \rangle \\ &- \frac{4\pi q'^2}{m(2\pi)^3} \int d^3p \tilde{n}(\mathbf{k}-\mathbf{p}) \frac{\mathbf{k}\cdot\mathbf{p}}{p^2} \delta\tilde{\rho}(\mathbf{p}, t) - \frac{4\pi q'^2}{m(2\pi)^3} \int d^3p \frac{\mathbf{k}\cdot\mathbf{p}}{p^2} \langle \Psi_{ion} | \delta\hat{\rho}(\mathbf{k}-\mathbf{p}) \delta\hat{\rho}(\mathbf{p}) | \Psi_{ion} \rangle. \end{aligned} \quad (10)$$

For small k , in analogy to the semiclassical approximation for electrons [19, 21], the contributions of the second and third components to the first term on the right-hand-side of Eq. (10) can be neglected as small in comparison to the first component. Small and thus negligible is also the third term in the right-hand-side of Eq.(10), as involving a product of two $\delta\tilde{\rho}$ (which we assumed small, $\delta\tilde{\rho}/n \ll 1$). This approach corresponds to the random-phase-approximation (RPA) formulated for bulk metal [20, 21]. Within the RPA, Eq. (10) attains the following shape,

$$\frac{\partial^2\delta\tilde{\rho}(\mathbf{k}, t)}{\partial t^2} = \frac{2k^2}{3m} \langle \Psi_{ion} | \sum_j e^{-i\mathbf{k}\cdot\mathbf{r}_j} \frac{\hbar^2 \nabla_j^2}{2m} | \Psi_{ion} \rangle - \frac{4\pi q'^2}{m(2\pi)^3} \int d^3p \tilde{n}(\mathbf{k}-\mathbf{p}) \frac{\mathbf{k}\cdot\mathbf{p}}{p^2} \delta\tilde{\rho}(\mathbf{p}, t), \quad (11)$$

and due to the spherical symmetry,

$$\langle \Psi_{ion} | \sum_j e^{-i\mathbf{k}\cdot\mathbf{r}_j} \frac{\hbar^2}{m^2} (\mathbf{k}\cdot\nabla_j)^2 | \Psi_{ion} \rangle \simeq \frac{2k^2}{3m} \langle \Psi_{ion} | \sum_j e^{-i\mathbf{k}\cdot\mathbf{r}_j} \frac{\hbar^2 \nabla_j^2}{2m} | \Psi_{ion} \rangle.$$

One can rewrite Eq. (11) in the position representation,

$$\begin{aligned} \frac{\partial^2\delta\tilde{\rho}(\mathbf{r}, t)}{\partial t^2} &= -\frac{2}{3m} \nabla^2 \langle \Psi_{ion} | \sum_j \delta(\mathbf{r}-\mathbf{r}_j) \frac{\hbar^2 \nabla_j^2}{2m} | \Psi_{ion} \rangle \\ &+ \frac{\omega_p^2}{4\pi} \nabla \left\{ \Theta(a-r) \nabla \int d^3r_1 \frac{1}{|\mathbf{r}-\mathbf{r}_1|} \delta\tilde{\rho}(\mathbf{r}_1, t) \right\}. \end{aligned} \quad (12)$$

In the case of metals it was next used the Thomas-Fermi formula to assess the averaged kinetic energy [20]:

$$\begin{aligned} \langle \Psi_{ion} | -\sum_j \delta(\mathbf{r}-\mathbf{r}_j) \frac{\hbar^2 \nabla_j^2}{2m} | \Psi_{ion} \rangle &\simeq \frac{3}{5} (3\pi^2)^{2/3} \frac{\hbar^2}{2m} (\rho(\mathbf{r}, t))^{5/3} \\ &= \frac{3}{5} (3\pi^2)^{2/3} \frac{\hbar^2}{2m} n^{5/3} \Theta(a-r) \left[1 + \frac{5}{3} \frac{\delta\tilde{\rho}(\mathbf{r}, t)}{n} + \dots \right]. \end{aligned} \quad (13)$$

The above Thomas-Fermi formula is addressed, however, to fermionic and degenerate quantum systems, as electrons in metals. For ionic systems such estimation of kinetic energy is inappropriate, because the ion concentration is usually much lower than that one of electrons in metals and the system is not degenerated even if ions are fermions. The Maxwell-Boltzmann distribution should be applied instead of the Fermi-Dirac or Bose-Einstein ones. Independently of fermionic or bosonic statistics of ions, the Maxwell-Boltzmann distribution allows for estimation of the averaged kinetic energy of ions located inside the sphere with the radius a , in the following form,

$$\langle \Psi_{ion} | -\sum_j \delta(\mathbf{r}-\mathbf{r}_j) \frac{\hbar^2 \nabla_j^2}{2m} | \Psi_{ion} \rangle \simeq (n + \delta\rho(\mathbf{r}, t)) \Theta(a-r) \frac{3kT}{2}, \quad (14)$$

where k is the Boltzmann constant and T is the temperature. For ions of the 3D shape or of the linear shape, the inclusion of rotational degrees of freedom would result in the factor $\frac{6kT}{2}$ or $\frac{5kT}{2}$, respectively, instead of $\frac{3kT}{2}$ for point like ion model.

Using the formula (14) and taking into account that $\nabla\Theta(a-r) = -\frac{\mathbf{r}}{r}\delta(a-r)$, one can rewrite Eq. (12) in the following manner,

$$\begin{aligned} \frac{\partial^2\delta\tilde{\rho}(\mathbf{r}, t)}{\partial t^2} &= \left[\frac{kT}{m} \nabla^2 \delta\tilde{\rho}(\mathbf{r}, t) - \omega_p^2 \delta\tilde{\rho}(\mathbf{r}, t) \right] \Theta(a-r) \\ &- \frac{kT}{m} \nabla \left\{ [n + \delta\tilde{\rho}(\mathbf{r}, t)] \frac{\mathbf{r}}{r} \delta(a-r) \right\} \\ &- \left[\frac{kT}{m} \frac{\mathbf{r}}{r} \nabla \delta\tilde{\rho}(\mathbf{r}, t) + \frac{\omega_p^2}{4\pi} \frac{\mathbf{r}}{r} \nabla \int d^3r_1 \frac{1}{|\mathbf{r}-\mathbf{r}_1|} \delta\tilde{\rho}(\mathbf{r}_1, t) \right] \delta(a-r). \end{aligned} \quad (15)$$

In the above formula ω_p is the bulk ion-plasmon frequency, $\omega_p^2 = \frac{4\pi n q'^2}{m}$. The solution of Eq. (15) can be decomposed into two parts related to the distinct domains—inside the sphere and on the sphere surface,

$$\delta\tilde{\rho}(\mathbf{r}, t) = \begin{cases} \delta\tilde{\rho}_1(\mathbf{r}, t), & \text{for } r < a, \\ \delta\tilde{\rho}_2(\mathbf{r}, t), & \text{for } r \geq a, (r \rightarrow a+), \end{cases} \quad (16)$$

corresponding to the volume and surface excitations, respectively. These two parts of ion local density fluctuations satisfy the equations (according to Eq. (15)),

$$\frac{\partial^2 \delta\tilde{\rho}_1(\mathbf{r}, t)}{\partial t^2} = \frac{kT}{m} \nabla^2 \delta\tilde{\rho}_1(\mathbf{r}, t) - \omega_p^2 \delta\tilde{\rho}_1(\mathbf{r}, t), \quad (17)$$

and (here $\epsilon = 0+$)

$$\begin{aligned} \frac{\partial^2 \delta\tilde{\rho}_2(\mathbf{r}, t)}{\partial t^2} = & -\frac{kT}{m} \nabla \left\{ [n + \delta\tilde{\rho}_2(\mathbf{r}, t)] \frac{\mathbf{r}}{r} \delta(a + \epsilon - r) \right\} \\ & - \left[\frac{kT}{m} \frac{\epsilon F}{m} \frac{\mathbf{r}}{r} \nabla \delta\tilde{\rho}_2(\mathbf{r}, t) + \frac{\omega_p^2}{4\pi} \frac{\mathbf{r}}{r} \nabla \int d^3 r_1 \frac{1}{|\mathbf{r} - \mathbf{r}_1|} (\delta\tilde{\rho}_1(\mathbf{r}_1, t) \Theta(a - r_1) + \delta\tilde{\rho}_2(\mathbf{r}_1, t) \Theta(r_1 - a)) \right] \delta(a + \epsilon - r). \end{aligned} \quad (18)$$

The Dirac delta in Eq. (18) results due to the derivative of the Heaviside step function—ideal jellium charge distribution. In Eq. (18) an infinitesimal shift, $\epsilon = 0+$, is introduced to fulfill requirements of the Dirac delta definition (its singular point must be an inner point of an open subset of the domain). This shift is only of a formal character and does not reflect any asymmetry.

The electric field due to surface charges is zero inside the sphere, and therefore cannot influence the volume excitations. Oppositely, the volume charge fluctuation-induced-electric-field can excite the surface fluctuations. Therefore, the equation for volume plasmons is independent of surface plasmons, whereas the volume plasmons contribute the equation for the surface plasmons.

The problem of separation between surface and volume plasmons has been thoroughly analyzed for metal clusters and was identified as significant for very small clusters. In the size-scale of 1 – 3 nm for metallic clusters, the effect of so-called spill-out of electrons beyond the jellium edge was important and caused the surface fuzzy resulting in coupling of volume and surface plasmon oscillations. Many direct numerical simulations (TDLDA, i.e., the time dependent local density approximation) [22, 23] have been verified that the volume–surface excitation miss-mass gradually disappears in larger clusters [22, 23], which supports accuracy of semiclassical RPA description, within which volume plasmons can be separated from the surface ones (even though the latter can be excited by the former ones, due to the last term in Eq. (18)). The quantum spill-out effect disappears gradually with growing sphere dimension and in the range of several nanometers for the metallic sphere radius is completely negligible. In the present paper we consider the radius range of ionic systems of micrometer order, when quantum effects are negligible. Such an opportunity allows us to formulate an analytical RPA semiclassical description in the form of an oscillator equation, allowing for phenomenological inclusion of the damping effects. The energy dissipation effects turned out to be overwhelming physical property in the case of larger metallic nanospheres [7, 19] (with $a > 10$ nm for Au or Ag) and also for much larger ionic systems, as we will demonstrate it below.

B. Solution of RPA equations: volume and surface plasmon frequencies

Eqs (17) and (18) are solved for metallic nanospheres [19] and these solutions can be directly applied to ionic systems. To summarize briefly this analysis, both parts of the plasma fluctuation can be represented as follows,

$$\begin{aligned} \delta\tilde{\rho}_1(\mathbf{r}, t) &= nF(\mathbf{r}, t), \quad \text{for } r < a, \\ \delta\tilde{\rho}_2(\mathbf{r}, t) &= \sigma(\Omega, t) \delta(r + \epsilon - a), \quad \epsilon = 0+, \quad \text{for } r \geq a, (r \rightarrow a+), \end{aligned} \quad (19)$$

with initial conditions, $F(\mathbf{r}, t)|_{t=0} = 0$, $\sigma(\Omega, t)|_{t=0} = 0$, (Ω is the spherical angle), $F(\mathbf{r}, t)|_{r=a} = 0$, $\int \rho(\mathbf{r}, t) d^3 r = N$ (neutrality condition). For the above initial and boundary conditions and taking advantage of the spherical symmetry, one can write out the time-dependent parts of the ion concentration fluctuations in the form [19] (cf. Appendix),

$$F(\mathbf{r}, t) = \sum_{l=1}^{\infty} \sum_{m=-l}^l \sum_{i=1}^{\infty} A_{lmn} j_l(k_{nl} r) Y_{lm}(\Omega) \sin(\omega_{li} t), \quad (20)$$

and

$$\begin{aligned} \sigma(\Omega, t) &= \sum_{l=1}^{\infty} \sum_{m=-l}^l \frac{B_{lm}}{a^2} Y_{lm}(\Omega) \sin(\omega_{0l} t) \\ &+ \sum_{l=1}^{\infty} \sum_{m=-l}^l \sum_{i=1}^{\infty} A_{lmn} \frac{(l+1)\omega_p^2}{l\omega_p^2 - (2l+1)\omega_{li}^2} Y_{lm}(\Omega) n_e \int_0^a dr_1 \frac{r_1^{l+2}}{a^{l+2}} j_l(k_{li} r_1) \sin(\omega_{li} t), \end{aligned} \quad (21)$$

where $j_l(\xi) = \sqrt{\frac{\pi}{2\xi}} I_{l+1/2}(\xi)$ is the spherical Bessel function, $Y_{lm}(\Omega)$ is the spherical function, $\omega_{li} = \omega_p \sqrt{1 + \frac{kT x_{li}^2}{\omega_p^2 a^2 m}}$ are the frequencies of the ion volume self-oscillations (volume plasmon frequencies), x_{li} are the nodes of the Bessel function $j_l(\xi)$ numerated with $i = 1, 2, 3, \dots$ (cf. Fig. 2), $k_{li} = x_{li}/a$, $\omega_{l0} = \omega_p \sqrt{\frac{l}{2l+1}}$ are the frequencies of the ion surface self-oscillations (surface plasmon frequencies). The derivation of the self-frequencies for ionic plasmon oscillations is presented with all the details in Appendix. Amplitudes A_{lmi} and B_{lm} are arbitrary in the homogeneous problem and can be adjusted to the initial conditions for the first derivatives.

The function $F(\mathbf{r}, t)$ describes volume plasmon oscillations, whereas $\sigma(\Omega, t)$ describes the surface plasmon oscillations. Let us emphasize that the first term in the Eq. (21) corresponds to the surface self-oscillations, while the second one term describes the surface oscillations induced by the volume plasmons. The frequencies of the surface self-oscillations are equal to,

$$\omega_{0l} = \omega_p \sqrt{\frac{l}{2l+1}}, \quad (22)$$

which, for $l = 1$, is the dipole type surface oscillation frequency, described for metallic nanosphere by Mie [24], $\omega_{01} = \omega_p/\sqrt{3}$.

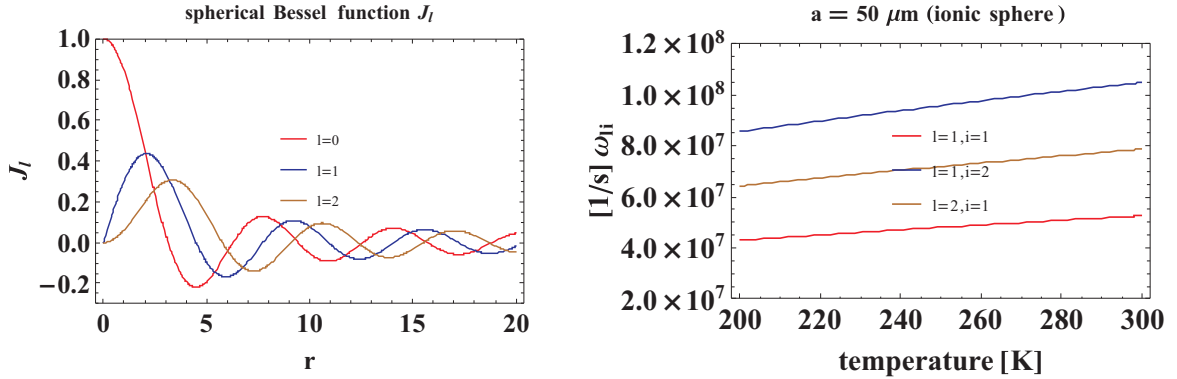


FIG. 2. The spherical Bessel functions $J_l(r)$ for $l = 0, 1, 2$ displaying possible charge density fluctuations in the sphere along the sphere radius r (arbitrary units) for volume plasmon modes; the angular distribution for these modes is governed by the real spherical functions $Y_{lm}(\Omega)$ similarly as for the surface plasmon modes (cf. Fig. 1 right). The exemplary temperature dependence of self-frequencies of volume plasmon modes ω_{li} , $li = 11, 12, 21$, for diluted electrolyte $n \simeq 10^{14} \text{ 1/m}^3$ and ion mass $\sim 10^4 m_e$, $a \sim 50 \mu\text{m}$ —right

C. Ionic surface plasmon frequencies for a nanosphere embedded in a dielectric medium, with $\epsilon_1 > 1$

One can now include the influence of a dielectric surroundings (in general, distinct from the inner one of considered ionic system) on plasmons in this system. In order to do it let us assume that ions on the surface ($r = a+$, i.e., $r \geq a$, $r \rightarrow a$) interact with Coulomb forces renormalized by the relative dielectric constant $\epsilon_1 > 1$ (distinct from ϵ for inner medium). Thus a small modification of Eq. (18) is of order,

$$\frac{\partial^2 \delta \tilde{\rho}_2(\mathbf{r})}{\partial t^2} = -\frac{2}{3m} \nabla \left\{ \left[\frac{3}{5} \epsilon_F n + \epsilon_F \delta \tilde{\rho}_2(\mathbf{r}, t) \right] \frac{\mathbf{r}}{r} \delta(a + \epsilon - r) \right\} - \left[\frac{2}{3} \frac{\epsilon_F}{m} \frac{\mathbf{r}}{r} \nabla \delta \tilde{\rho}_2(\mathbf{r}, t) + \frac{\omega_p^2}{4\pi} \frac{\mathbf{r}}{r} \nabla \int d^3 r_1 \frac{1}{|\mathbf{r} - \mathbf{r}_1|} \left(\delta \tilde{\rho}_1(\mathbf{r}_1, t) \Theta(a - r_1) + \frac{1}{\epsilon_1} \delta \tilde{\rho}_2(\mathbf{r}_1, t) \Theta(r_1 - a) \right) \right] \delta(a + \epsilon - r), \quad (23)$$

(note that Eq. (17) is not affected by the outer medium). The solution of the above equation is of the same form as that one for the Eq. (18) case, but with the renormalized surface plasmon frequencies,

$$\omega_{0l} = \omega_p \sqrt{\frac{l}{2l+1} \frac{1}{\epsilon_1}}. \quad (24)$$

III. DAMPING OF PLASMON OSCILLATIONS IN IONIC SYSTEMS

The semiclassical RPA treatment of plasmon excitations in finite ion systems as presented above, does not account for plasmon damping. The damping of plasmon oscillations can be, however, included in a phenomenological manner, by addition of an attenuation term to plasmon dynamic equations, i.e., the term, $-\frac{2}{\tau_0} \frac{\partial \delta \rho(\mathbf{r}, t)}{\partial t}$, added to the right hand sides of both Eqs (17) and (18), taking into account their oscillatory form. The introduced damping ratio $\frac{1}{\tau_0}$ accounts for ion scattering losses and can be approximated in analogy to metallic systems, by inclusion of energy dissipation caused by irreversible its transformation into heat via various microscopic channels similar to those for Ohmic resistivity [25],

$$\frac{1}{\tau_0} \simeq \frac{v}{2\lambda_b} + \frac{Cv}{2a}, \quad (25)$$

where a is the sphere radius, v is the mean velocity of ions, $v = \sqrt{\frac{3kT}{m}}$, λ_b is the ion mean free path in bulk electrolyte material the same as the sphere is made of (including scattering of ions on other ions, and on solvent particles and admixtures). The second term in Eq. (25) accounts for scattering of ions on the boundary of the finite ionic system, the sphere with the radius a , the constant C is of order of unity [25].

In order to explicitly express a forcing field which moves ions in the system, the inhomogeneous time dependent term should be added to the homogeneous equations (17) and (18). The forcing field may be the time dependent electric field. If one considers it as the electric component of the incident e-m wave then the comparison of the resonant wave-length with the system size is of order. Similarly as for metallic nano-spheres also for finite ionic systems the surface plasmon resonant wave-length highly exceeds the system dimension and the forcing field is practically uniform along whole the system. Such a perturbation could excite only surface dipole plasmons, i.e., the mode with $l = 1$, which can be described by the function $Q_{1m}(t)$ ($l = 1$ and m are angular momentum numbers related to the assumed spherical symmetry of the system). The corresponding dynamical equation for surface plasmons reduced to only mode $Q_{1m}(t)$ has the following form,

$$\begin{aligned} & \frac{\partial^2 Q_{1m}(t)}{\partial t^2} + \frac{2}{\tau_0} \frac{\partial Q_{1m}(t)}{\partial t} + \omega_1^2 Q_{1m}(t) \\ & = \sqrt{\frac{4\pi}{3}} \frac{qn}{m} [E_z(t)\delta_{m,0} + \sqrt{2}(E_x(t)\delta_{m,1} + E_y(t)\delta_{m,-1})], \end{aligned} \quad (26)$$

where $\omega_1 = \frac{\omega_p}{\sqrt{3\varepsilon_1}}$ (it is a dipole surface plasmon frequency, i.e., the Mie frequency [24], ε_1 is the dielectric susceptibility of the system surroundings). Because only Q_{1m} contribute to the plasmon response to the homogeneous electric field, thus the effective ion density fluctuation has the form [19],

$$\delta\rho(\mathbf{r}, t) = \begin{cases} 0, & r < a, \\ \sum_{m=-1}^1 Q_{1m}(t) Y_{1m}(\Omega) & r \geq a, r \rightarrow a+, \end{cases} \quad (27)$$

where $Y_{lm}(\Omega)$ is the spherical function with $l = 1$. One can also explicitly calculate the dipole $\mathbf{D}(t)$ corresponding to surface plasmon oscillations given by Eq. (27),

$$\begin{cases} D_x(t) = q' \int d^3r x \delta\rho(\mathbf{r}, t) = \frac{\sqrt{2\pi}}{\sqrt{3}} q' Q_{1,1}(t) a^3, \\ D_y(t) = q' \int d^3r y \delta\rho(\mathbf{r}, t) = \frac{\sqrt{2\pi}}{\sqrt{3}} q' Q_{1,-1}(t) a^3, \\ D_z(t) = q' \int d^3r z \delta\rho(\mathbf{r}, t) = \frac{\sqrt{4\pi}}{\sqrt{3}} q' Q_{1,0}(t) a^3. \end{cases} \quad (28)$$

The dipole $\mathbf{D}(t)$ satisfies the equation (it is rewritten Eq. (26)),

$$\left[\frac{\partial^2}{\partial t^2} + \frac{2}{\tau_0} \frac{\partial}{\partial t} + \omega_1^2 \right] \mathbf{D}(t) = \frac{a^3 4\pi q'^2 n}{3m} \mathbf{E}(t) = \varepsilon a^3 \omega_1^2 \mathbf{E}(t). \quad (29)$$

One can notice that the dipole (28) scales as the system volume, $\sim a^3$, which may be interpreted that all ions actually contribute to the surface plasmon oscillations. This is connected with the fact that the surface modes correspond to uniform translation-type oscillations of ions in the system, when inside the sphere the charge of ions is exactly compensated by oppositely signed ions, whereas the not balanced charge density occurs only on the surface despite all ions oscillate. For the volume plasmons the non-compensated charge density fluctuations are present also inside

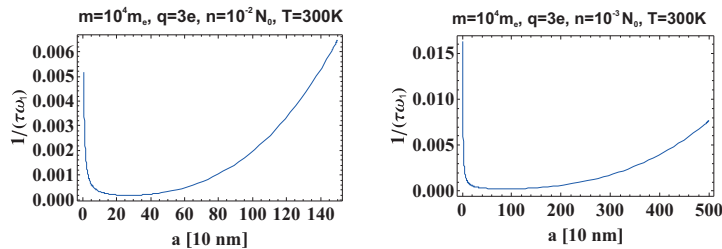


FIG. 3. The cross-over in ionic system-size dependence of damping rate for surface plasmons, for $T = 300K$, $m = 10^4 m_e$, $q = 3e$, $n = 10^{-2} N_0$ (N_0 is the concentration of one molar electrolyte) (left) and for $n = 10^{-3} N_0$ (right); in the size-region close to the cross-over the perturbative treatment for Lorentz friction perfectly coincides with the exact approach

the sphere as volume plasmon modes have the compressional character with not balanced charge fluctuations along the system radius.

The scattering effects accounted for by the approximate formula (25) cause damping of plasmons especially strong for small size of the system due to the nanosphere-edge scattering contribution proportional to $\frac{1}{a}$. This term is, however, of lowering significance with the radius growth. We will show that radiation losses resulted due to accelerated movement of ions scales as a^3 , and for rising a these irradiative energy losses quickly dominate plasmon attenuation. Due to opposite size dependence of scattering and irradiation contributions to the plasmon damping one can thus observe the cross-over in dumping with respect to its size dependence, as it is depicted in Fig. 3. One can also determine the radius a^* for which the total attenuation rate for surface plasmons is minimal, $a^* = \left(\frac{3^{3/2} C c^3 v}{2 \omega_1 \omega_p^3} \right)^{1/4}$. The system sizes a^* for two distinct ionic systems are listed in Tab. I.

The irradiation of energy of the oscillating dipole is expressed by the so-called Lorentz friction [16], i.e., the effective electric field slowing down the motion of charges,

$$\mathbf{E}_L = \frac{2\sqrt{\varepsilon}}{3c^3} \frac{\partial^3 \mathbf{D}(t)}{\partial t^3}. \quad (30)$$

Hence, we can rewrite Eq. (29) including the Lorentz friction term,

$$\left[\frac{\partial^2}{\partial t^2} + \frac{2}{\tau_0} \frac{\partial}{\partial t} + \omega_1^2 \right] \mathbf{D}(t) = \varepsilon a^3 \omega_1^2 \mathbf{E}(t) + \varepsilon a^3 \omega_1^2 \mathbf{E}_L, \quad (31)$$

or for $\mathbf{E} = 0$,

$$\left[\frac{\partial^2}{\partial t^2} + \omega_1^2 \right] \mathbf{D}(t) = \frac{\partial}{\partial t} \left[-\frac{2}{\tau_0} \mathbf{D}(t) + \frac{2}{3\omega_1} \left(\frac{\omega_p a}{c\sqrt{3}} \right)^3 \frac{\partial^2}{\partial t^2} \mathbf{D}(t) \right]. \quad (32)$$

One can apply the perturbation method for solution of Eq. (32) when the right hand side of this equation is treated as a small perturbation. In the zeroth step of the perturbation we have $\left[\frac{\partial^2}{\partial t^2} + \omega_1^2 \right] \mathbf{D}(t) = 0$, from which $\frac{\partial^2}{\partial t^2} \mathbf{D}(t) = -\omega_1^2 \mathbf{D}(t)$. Hence, for the first step of the perturbation, we put the latter formula to the right hand side of Eq. (32), i.e.,

$$\left[\frac{\partial^2}{\partial t^2} + \frac{2}{\tau} \frac{\partial}{\partial t} + \omega_1^2 \right] \mathbf{D}(t) = 0, \quad (33)$$

where

$$\frac{1}{\tau} = \frac{1}{\tau_0} + \frac{\omega_1}{3} \left(\frac{\omega_p a}{c\sqrt{3}} \right)^3. \quad (34)$$

Within the first step of perturbation, the Lorentz friction can be included into the total attenuation rate $\frac{1}{\tau}$. Nevertheless, this approximation is justified only for sufficiently small perturbations, i.e., when the second term in Eq. (34), proportional to a^3 , is small enough to fulfill the perturbation restrictions. The related limiting value, \tilde{a} , of the ionic system size depends on the ion concentration, charge, mass, dielectric susceptibility, as is exemplified below in the following subsection.

The solution of Eq. (33) is of the form $\mathbf{D}(t) = \mathbf{A}e^{-t/\tau} \cos(\omega'_1 t + \phi)$, where $\omega'_1 = \omega'_1 \sqrt{1 - \frac{1}{(\omega_1 \tau)^2}}$, which gives the red shift of the plasmon resonance due to strong, $\sim a^3$, growth of attenuation caused by the irradiation. The Lorentz friction term in Eq. (34) dominates plasmon damping for $a \leq \tilde{a}$ due to this a^3 dependence—cf. Fig. 3. The plasmon damping grows rapidly with a and this results in pronounced redshift of resonance frequency.

A. Exact inclusion of the Lorentz damping to the attenuation of ionic dipole surface plasmons

Now we will consider the dynamic equation for surface plasmons in the ionic spherical system (32) with the Lorentz friction term, but without application of the perturbation method for solution resulting in substitution of the Lorentz friction term $\frac{2}{3\omega_1} \left(\frac{\omega_p a}{v\sqrt{3}}\right)^3 \frac{\partial^3 \mathbf{D}(t)}{\partial t^3}$ with the approximate formula, $-\frac{2\omega_1}{3} \left(\frac{\omega_p a}{v\sqrt{3}}\right)^3 \frac{\partial \mathbf{D}(t)}{\partial t}$, what was the result of taking in the right hand side of Eq. (32) the zeroth order its solution, for which $\frac{\partial^2 \mathbf{D}(t)}{\partial t^2} = -\omega_1^2 \mathbf{D}(t)$. To compare various contributions to Eq. (32) we change to dimensionless variable $t \rightarrow t' = \omega_1 t$. Then Eq. (32) attains the form,

$$\frac{\partial^2 \mathbf{D}(t')}{\partial t'^2} + \frac{2}{\tau_0 \omega_1} \frac{\partial \mathbf{D}(t')}{\partial t'} + \mathbf{D}(t') = \frac{2}{3} \left(\frac{\omega_p a}{v\sqrt{3}}\right)^3 \frac{\partial^3 \mathbf{D}(t')}{\partial t'^3}. \quad (35)$$

In the case of solution of Eq. (35) by perturbation we get renormalized attenuation rate for effective damping term, $\frac{1}{\omega_1 \tau_0} + \frac{1}{3} \left(\frac{\omega_p a}{v\sqrt{3}}\right)^3$. This term quickly achieves the value 1, for which the oscillator falls into the over-damped regime. For system parameters as assumed for Fig. 3, the achievement by the attenuation rate of the value equal 1 takes place at 25,5 μm and 8 μm for $n = 10^{-3} N_0$ and $n = 10^{-2} N_0$, respectively. At these values of a , the frequency $\omega'_1 = \omega'_1 \sqrt{1 - \frac{1}{(\omega_1 \tau)^2}}$ goes to zero, which indicates an apparent artifact of the perturbation method. To verify how behaves the exact damped frequency in the considered system one has to solve the dynamical equation without any approximations. As this equation is of third order linear differential equation, one can find its solution in the form, $\sim e^{i\Omega t'}$, with the analytical expressions for three possible values of the exponent,

$$\begin{aligned} \Omega_1 &= -\frac{i}{3g} - \frac{i2^{1/3}(1+6gu)}{3g(2+27g^2+18gu+\sqrt{4(-1-6gu)^3+(2+27g^2+18gu)^2})^{1/3}} \\ &\quad - \frac{i(2+27g^2+18gu+\sqrt{4(-1-6gu)^3+(2+27g^2+18gu)^2})^{1/3}}{3 \times 2^{1/3}g} \in \text{Im}(= i\alpha), \\ \Omega_2 &= -\frac{i}{3g} + \frac{i(1+i\sqrt{3})(1+6gu)}{3 \times 2^{2/3}g(2+27g^2+18gu+\sqrt{4(-1-6gu)^3+(2+27g^2+18gu)^2})^{1/3}} \\ &\quad + \frac{i(1-i\sqrt{3})(2+27g^2+18gu+\sqrt{4(-1-6gu)^3+(2+27g^2+18gu)^2})^{1/3}}{6 \times 2^{1/3}g} = \omega + i\frac{1}{\tau}, \\ \Omega_3 &= -\frac{i}{3g} + \frac{i(1-i\sqrt{3})(1+6gu)}{3 \times 2^{2/3}g(2+27g^2+18gu+\sqrt{4(-1-6gu)^3+(2+27g^2+18gu)^2})^{1/3}} \\ &\quad + \frac{i(1+i\sqrt{3})(2+27g^2+18gu+\sqrt{4(-1-6gu)^3+(2+27g^2+18gu)^2})^{1/3}}{6 \times 2^{1/3}g} = -\omega + i\frac{1}{\tau}, \end{aligned} \quad (36)$$

where $u = \frac{1}{\tau_0 \omega_1}$ and $g = 2/3 \left(\frac{a\omega_p}{c\sqrt{3}\epsilon_1}\right)^3$.

In Fig. 4 we have plotted the damping rate ($\text{Im}\Omega$) and the self-frequency ($\text{Re}\Omega$) (also translated for resonance wavelength—right pannels) with respect to the system radius a . For comparison, the approximate perturbative solutions are plotted also—the blue line, whereas the exact solution of Eq. (35) is plotted in red line. The blue line finishes at a_{limit} , when the attenuation rate within the perturbation approach reaches the critical value 1 (then $\lambda \rightarrow \infty$). For the accurate solution of Eq. (35) this singular behavior disappears and the oscillating solution, $e^{i\Omega t}$, exists for larger a as well.

We notice that the red-shift of the plasmon resonance is strongly overestimated in the framework of the perturbative approach to the Lorentz friction unless $a < \tilde{a}$, where \tilde{a} is sensitive to ionic system parameters and especially to ion concentration (as is demonstrated in Fig. 4).

Let us emphasize that the equation (35) has in general two types of particular solutions, $e^{i\Omega t'}$, with complex self-frequencies Ω . The solutions given by Ω_2 and Ω_3 are of oscillating type with damping ($i\Omega_2$ and $i\Omega_3$ are mutually conjugated, thus Ω_2 and Ω_3 have the real parts of opposite sign, whereas the same imaginary parts, the latter is positive displaying the damping rate) and the second one—given by Ω_1 , which turns out to be an unstable exponentially rising solution (negative imaginary solution). This unstable solution is the well known artifact in the Maxwell electrodynamics (cf. e.g., § 75 in [16]) and corresponds to the infinite self-acceleration of the free charge due to

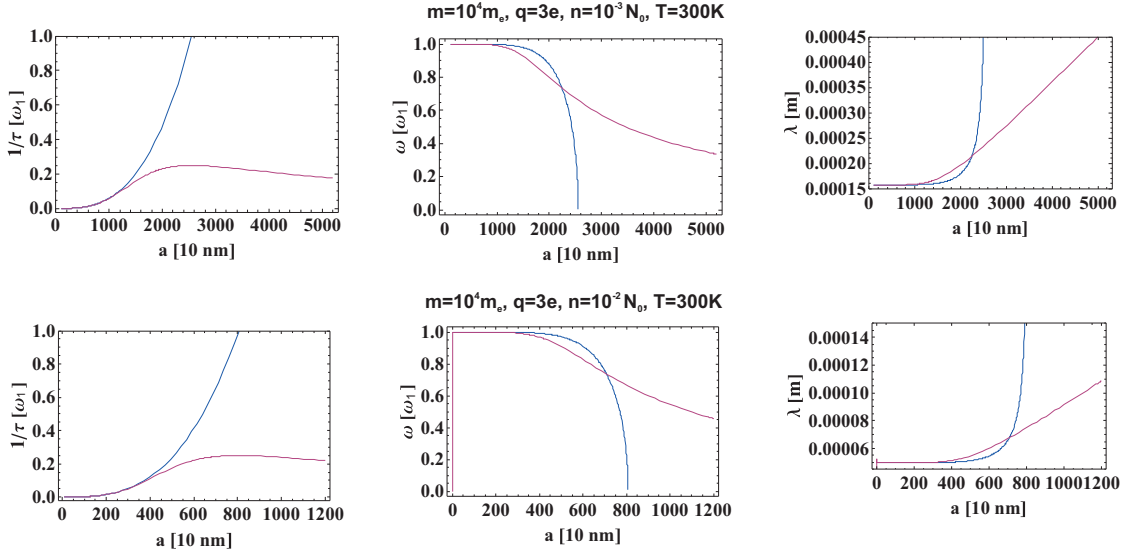


FIG. 4. Comparison of the damping rate and the resonance frequency (transformed also into the resonance wave-length—in right panels), i.e., the damping rate and frequency (wave length) of oscillating solution of Eq.(35), exact (red line) and approximate upon perturbation approach (blue line), both with respect to the ionic finite system radius a

material	ionic system	sample 1	sample 2
ion concentration	n (N_0 is one-molar concentr.)	$10^{-2} N_0$	$10^{-3} N_0$
effective ion mass	m (m_e electron mass)	$10^4 m_e$	$10^4 m_e$
charge of effective ion	$q/\sqrt{\epsilon}$	$3 e$	$3 e$
temperature	T	300 K	300 K
mean velocity of ions	$v = \sqrt{\frac{3kT}{m}}$	1168 m/s	1168 m/s
bulk plasmon frequency	ω_p	9.3×10^{13} 1/s	2.93×10^{12} 1/s
dielectric constant of surroundings	ϵ_1	2	2
Mie frequency	$\omega_1 = \omega_p/\sqrt{3\epsilon_1}$	3.8×10^{13} 1/s	1.2×10^{12} 1/s
constant in Eq. (25)	C	2	2
bulk mean free path (room temp.)	λ_b	$0.5 \mu\text{m}$	$0.1 \mu\text{m}$
radius for minimal damping	$a^* = \left(\frac{3^{3/2} C c^3 v}{2\omega_1 \omega_p^3}\right)^{1/4}$	2.7×10^{-7} m	8.6×10^{-7} m

TABLE I. The ion-system parameters assumed for calculation of damping rates and self-frequency for dipole surface plasmons

Lorentz friction force (i.e., to the singular solution of the equation $m\dot{\mathbf{v}} = \text{const.} \times \dot{\mathbf{v}}$, which is associated with a formal renormalization of the field-mass of the charge—infinite for point-like charge and canceled in an artificial manner by arbitrary assumed negative infinite non-field mass, resulting in ordinary mass of e.g., an electron, which is, however, not defined mathematically in a proper way). This unphysical singular particular solution should be thus discarded. The other oscillatory type solution resembles the solution of the ordinary damped harmonic oscillator, though with distinct attenuation rate and frequency. They are expressed by analytical formulae for Ω_2 and Ω_3 by Eqs (36) and then are calculated for various a and compared with the corresponding quantities found within the perturbation approach. This comparison is presented in Fig. 4. From this comparison it is clearly visible that application of the perturbation approach leads to high overestimation of the damping rate for $a > \tilde{a}$. Therefore, we can conclude that the usage of the approximate formula for the Lorentz friction damping in the form (34) is justified up to $a \simeq \tilde{a}$, while for $a > \tilde{a}$, these approximate values strongly differ from the exact ones. The value $\tilde{a} < a_{limit}$ sharply depends on ionic system parameters and approximately $\tilde{a} \simeq \frac{a_{limit}}{2}$.

IV. CONCLUSIONS

Concluding, we can state that in ionic finite systems we may observe plasmons similar as in the metallic nanoparticles. The structure of surface and volume plasmons for ions is repeated from the similar properties of electronic plasmons in metallic spherical systems, however, with the significant shift of resonant energy towards lower one correspondingly to by few orders larger mass of ions in comparison to electron mass and different concentration of ions in electrolyte. Thus corresponding to the resonant energy electro-magnetic wave length is shifted to deep infra-red or even longer wave lengths depending on ion concentration. The typical for metal clusters cross-over in size dependence of plasmon damping between the scattering, leading to Ohmic type energy dissipation, versus the irradiation losses also is observable in ionic spherical system with similar to metal size-dependence, though shifted toward the micrometer scale for ions instead on the nanometer scale for metals. Of particular interest is the high irradiation regime for dipole plasmons in ionic system with prospective application for signaling and energy transfer in ionic systems. The initial strong enhancement of efficiency of the Lorentz friction with the radius growth of electrolyte sphere is observed on the micrometer scale with typical a^3 radius dependence above some threshold radius which value depends on electrolyte parameters. At certain value of the radius (varying in a wide range also depending on ion system parameters) this enhancement saturates and then the irradiation losses slowly diminish, which allows for definition of the most convenient sizes of electrolyte finite system for optimizing radiation mediated transport efficiency preferring the highest radiation losses.

Acknowledgments Authors acknowledge the support of the present work upon the NCN project no. 2011/03/D/ST3/02643 and the NCN project no. 2011/02/A/ST3/00116.

Appendix A: Derivation of plasmon frequencies

1. Volume plasmons

In order to determine self-frequencies of the volume ionic plasmon in the sphere we must solve Eq. (17) with the form of the relevant solution given by Eq. (19). For initial conditions listed below Eq. (19) we assume $F(\mathbf{r}, t) = F_\omega(\mathbf{r})\sin(\omega t)$ and by substitution of this function into Eq. (17) we get,

$$\Delta F_\omega(\mathbf{r}) + k^2 F_\omega(\mathbf{r}) = 0, \quad (\text{A1})$$

where $k^2 = \frac{(\omega^2 - \omega_p^2)m}{kT}$. This is a well known Helmholtz differential equation of which solutions (finite in the origin) can be expressed by the spherical Bessel functions (for the radial dependence of $F_\omega(\mathbf{r})$),

$$F_\omega(\mathbf{r}) = A j_l(kr) Y_{lm}(\Omega), \quad (\text{A2})$$

where $j_l(x) = \sqrt{\frac{\pi}{2x}} I_{l+1/2}(x)$ is the the l th spherical Bessel function linked to the Bessel function of first kind. The boundary condition, $F(a) = 0$, gives quantization of k , $k_{li} = \frac{x_{li}}{a}$, where x_{li} is the i th zero of the l th Bessel function (cf. Fig. 2 left). Following this quantization one arrives at the corresponding self-frequency quantization,

$$\omega_{li}^2 = \omega_p^2 \left(1 + \frac{kT x_{li}}{\omega_p^2 m a^2} \right). \quad (\text{A3})$$

Thus the volume ionic plasmons in the sphere are described by functions,

$$\delta\rho_1(\mathbf{r}, t) = n \sum_{l=1}^{\infty} \sum_{m=-l}^{m=l} \sum_{i=1}^{\infty} A_{lmi} j_l(k_{li}r) Y_{lm}(\Omega) \sin(\omega_{li}t), \quad (\text{A4})$$

where A_{lmi} are arbitrary constants. The component with $l = 0$ vanishes because of neutrality condition, $\int_0^a r^2 dr d\Omega F(\mathbf{r}, t) = 0$ (as $\int d\Omega Y_{lm}(\Omega) = \sqrt{4\pi} \delta_{l0} \delta_{m0}$, $d\Omega = \sin\Theta d\Theta d\phi$). Note that in ionic systems self-frequencies of volume plasmons in the sphere are temperature dependent—cf Eq. (A3) and Fig. 2 right.

2. Surface plasmons

In order to determine self-frequencies for surface plasmons, one has to consider Eq. (18) and solution for it given by Eq. (19). The first term in the right hand side of Eq. (18) can be rewritten to the form,

$$\begin{aligned} & \frac{kT}{m} \nabla(n + \delta\rho_2) \nabla \Theta(a - r) + \frac{kT}{m} (n + \delta\rho) \Delta \Theta \\ &= -\frac{kT}{m} \delta(a - r) \frac{\partial}{\partial r} (n + \delta\rho) = \frac{kT}{m} \frac{1}{r^2} \frac{\partial}{\partial r} (r^2 \delta(a - r)) \\ &= -\frac{kT}{m} \frac{1}{r^2} \frac{\partial}{\partial r} [(n + \delta\rho_2) r^2 \delta(a - r)], \end{aligned} \quad (\text{A5})$$

where we used formulae $\nabla \Theta(a - r) = -\frac{\mathbf{r}}{r} \delta(a - r)$, $\frac{\mathbf{r}}{r} \nabla = \frac{\partial}{\partial r}$. The next term in the right hand side of Eq. (18) can be transformed into,

$$\begin{aligned} & -\frac{kT}{m} \delta(a - r) \frac{\mathbf{r}}{r} \nabla \delta\rho_2 - \frac{\omega_p^2}{4\pi} \delta(a - r) \frac{\mathbf{r}}{r} \nabla \int \frac{d^3 r_1 \delta\rho(\mathbf{r}_1)}{|\mathbf{r} - \mathbf{r}_1|} \\ &= -\frac{kT}{m} \delta(a - r) \frac{\partial}{\partial r} \delta\rho - 2 - \frac{\omega_p^2}{4\pi} \delta(a - r) \frac{\partial}{\partial r} \int \frac{d^3 r_1 \delta\rho(\mathbf{r}_1)}{|\mathbf{r} - \mathbf{r}_1|}. \end{aligned} \quad (\text{A6})$$

Eq. (18) attains thus the form,

$$\begin{aligned} \frac{\partial^2 \rho_2}{\partial t^2} &= -\frac{kT}{m} \frac{1}{r^2} \frac{\partial}{\partial r} [(n + \delta\rho_2) r^2 \delta(a - r)] \\ &- \frac{kT}{m} \delta(a - r) \frac{\partial}{\partial r} \delta\rho - 2 - \frac{\omega_p^2}{4\pi} \delta(a - r) \frac{\partial}{\partial r} \int \frac{d^3 r_1 \delta\rho(\mathbf{r}_1)}{|\mathbf{r} - \mathbf{r}_1|}. \end{aligned} \quad (\text{A7})$$

We suppose the solution of the above equation in the form, $\delta\rho_2 = \sigma(\Omega, t) \delta(a + 0^+ - r)$ and multiply both sides of this equation by r^2 and integrate with respect to r in arbitrary limits, i.e., $\int_l^L r^2 dr \dots$, such that $a \in (l, L)$ (this integration removes Dirac deltas), which leads to the equation,

$$\begin{aligned} a^2 \frac{\partial^2 \sigma(\Omega, t)}{\partial t^2} &= -\frac{kT}{m} \int_l^L dr \frac{\partial}{\partial r} [(n + \delta\rho_2) r^2 \delta(a - r)] \\ &- \frac{kT}{m} \sigma(\Omega, t) \int_l^L r^2 dr \delta(a - r) \frac{\partial}{\partial r} \delta(a - r) \\ &- \frac{\omega_p^2}{4\pi} \int_l^L r^2 dr \delta(a - r) \frac{\partial}{\partial r} \int_a^\infty r_1^2 dr_1 \int d\Omega \frac{\delta\rho_1(\mathbf{r}_2)}{|\mathbf{r} - \mathbf{r}_1|} \\ &- \frac{\omega_p^2}{4\pi} \int_l^L r^2 dr \delta(a - r) \frac{\partial}{\partial r} \int_0^a r_1^2 dr_1 \int d\Omega \frac{\delta\rho_1(\mathbf{r}_1)}{|\mathbf{r} - \mathbf{r}_1|}. \end{aligned} \quad (\text{A8})$$

Two first terms in the right hand side of the above equation vanish, because,

$$-\frac{kT}{m} \int_l^L dr \frac{\partial}{\partial r} [(n + \delta\rho_2) r^2 \delta(a - r)] = -\frac{kT}{m} [(n + \delta\rho_2) r^2 \delta(r - a)] \Big|_l^L = 0 \quad (\text{A9})$$

and

$$\begin{aligned} & -\frac{kT}{m} \sigma(\Omega, t) \int_l^L r^2 dr \delta(a - r) \frac{\partial}{\partial r} \delta(a - r) = -\frac{kT}{m} a^2 \int_l^L dr \frac{1}{2} \frac{\partial}{\partial r} \delta^2(a - r) \\ &= -\frac{kT}{m} \frac{a^2}{2} \delta^2(a - r) \Big|_l^L = -\frac{kT}{m} \frac{a^2}{2} \lim_{\mu \rightarrow 0} \frac{1}{\pi} \frac{\mu}{\mu^2 + (a - r)^2} \delta(a - r) \Big|_l^L = 0. \end{aligned} \quad (\text{A10})$$

Two last terms of r.h.s. of Eq. (A8) can be transformed using the formula [26], $\frac{1}{\sqrt{1+z^2-2z\cos\gamma}} = \sum_{l=0}^{\infty} P_l(\cos\gamma) z^l$, for $z < 1$, where $P_l(\cos\gamma) = \frac{4\pi}{2l+1} \sum_{m=-l}^l Y_{lm}(\Omega) Y_{lm}^*(\Omega)$ are Legendre polynomials. This formula leads to the following one,

$$\frac{\partial}{\partial a} \frac{1}{|\mathbf{a} - \mathbf{r}_1|} = \begin{cases} \sum_{l=0}^{\infty} \frac{l a^{l-1}}{r_1^{l+1}} P_l(\cos\gamma), & \text{for } a < r_1, \\ -\sum_{l=0}^{\infty} \frac{(l+1) r_1^l}{a^{l+2}} P_l(\cos\gamma), & \text{for } a > r_1, \end{cases} \quad (\text{A11})$$

where $\mathbf{a} = a \frac{\mathbf{r}}{r}$, $\cos\gamma = \frac{\mathbf{a} \cdot \mathbf{r}_1}{ar_1}$. Employing Eq. (A11), the last two terms in Eq. (A8) can be transformed as follows,

$$\begin{aligned}
& -\frac{\omega_p^2}{4\pi} \int_l^L r^2 dr \delta(a-r) \frac{\partial}{\partial r} \int_a^\infty r_1^2 dr_1 \int d\Omega_1 \frac{\delta\rho_2(\mathbf{r}_1)}{|\mathbf{r}-\mathbf{r}_1|} \\
& = -\frac{\omega_p^2}{4\pi} a^2 \int d\Omega_1 \int_a^\infty r_1^2 dr_1 \delta\rho_2(\mathbf{r}_1) \frac{\partial}{\partial a} \frac{1}{\sqrt{a^2+r_1^2-2ar_1\cos\gamma}} \\
& = -\frac{\omega_p^2}{4\pi} a^2 \int d\Omega_1 \int_a^\infty r_1^2 dr_1 \sigma(\Omega_1) \delta(a+0+-r_1) \sum_{l=0}^\infty \frac{l a^{l-1}}{r_1^{l+1}} P_l(\cos\gamma) \\
& = -\frac{\omega_p^2}{4\pi} a^2 \int d\Omega_1 \sigma(\Omega_1) \frac{1}{a^2} \sum_{l=0}^\infty \frac{4\pi l}{2l+1} \sum_{m=-l}^l Y_{lm}(\Omega) Y_{lm}^*(\Omega_1) \\
& = -\omega_p^2 a^2 \sum_{l=0}^\infty \sum_{m=-l}^l \frac{l}{2l+1} Y_{lm}(\Omega) \int d\Omega_1 \sigma(\Omega_1) Y_{lm}^*(\Omega_1),
\end{aligned} \tag{A12}$$

and

$$\begin{aligned}
& -\frac{\omega_p^2}{4\pi} \int_l^L r^2 dr \delta(a-r) \frac{\partial}{\partial r} \int_0^a r_1^2 dr_1 \int d\Omega_1 \frac{\delta\rho_1(\mathbf{r}_1)}{|\mathbf{r}-\mathbf{r}_1|} \\
& = -\frac{\omega_p^2}{4\pi} a^2 \int d\Omega_1 \int_0^a r_1^2 dr_1 n F(\mathbf{r}_1, t)(\mathbf{r}_1) \frac{\partial}{\partial a} \frac{1}{\sqrt{a^2+r_1^2-2ar_1\cos\gamma}} \\
& = \frac{\omega_p^2}{4\pi} a^2 \int d\Omega_1 n F(\mathbf{r}_1, t) \sum_{l=0}^\infty \frac{(l+1)r_1^l}{a^{l+2}} P_l(\cos\gamma) \\
& = \omega_p^2 n \sum_{l=0}^\infty \sum_{i=0}^l \frac{l+1}{2l+1} Y_{lm}(\Omega) \int_0^a r_1^2 dr_1 \frac{r_1^l}{a^l} \sum_{l_1=1}^l \sum_{m_1=-l_1}^{l_1} \sum_i A_{lmi} j_{l_1}(k_{l_1} r_1) \sin(\omega_{l_1} t) \int d\Omega_1 Y_{lm}^*(\Omega_1) Y_{l_1 m_1}(\Omega_1) \\
& = \omega_p^2 n \sum_{l=0}^\infty \sum_{m=-l}^l \sum_i \frac{l+1}{2l+1} Y_{lm}(\Omega) A_{lmi} \int_0^a \frac{r_1^{l+2} dr_1}{a^l} j_l(k_{li} r_1) \sin(\omega_{li} t).
\end{aligned} \tag{A13}$$

Equation (A8) attains thus the form,

$$\begin{aligned}
\frac{\partial^2 \sigma(\Omega, t)}{\partial t^2} & = -\omega_p^2 a^2 \sum_{l=0}^\infty \sum_{m=-l}^l \frac{l}{2l+1} Y_{lm}(\Omega) \int d\Omega_1 \sigma(\Omega_1) Y_{lm}^*(\Omega_1) \\
& + \omega_p^2 n \sum_{l=0}^\infty \sum_{m=-l}^l \sum_i \frac{l+1}{2l+1} Y_{lm}(\Omega) A_{lmi} \int_0^a \frac{r_1^{l+2} dr_1}{a^l} j_l(k_{li} r_1) \sin(\omega_{li} t),
\end{aligned} \tag{A14}$$

Assuming now, $\sigma(\Omega, t) = \sum_{l=0}^\infty \sum_{m=-l}^l q_{lm}(t) Y_{lm}(\Omega)$ and putting it to the above equation, we obtain,

$$\begin{aligned}
\sum_{l=0}^\infty \sum_{m=-l}^l Y_{lm}(\Omega) \frac{\partial^2 q_{lm}(t)}{\partial t^2} & = -\sum_{l=0}^\infty \sum_{m=-l}^l \frac{\omega_p^2 l}{2l+1} Y_{lm}(\Omega) q_{lm}(t) \\
& + \omega_p^2 n \sum_{l=1}^\infty \sum_{m=-l}^l \sum_i \frac{l+1}{2l+1} Y_{lm}(\Omega) A_{lmi} \int_0^a \frac{r_1^{l+2} dr_1}{a^{l+2}} j_l(k_{li} r_1) \sin(\omega_{li} t).
\end{aligned} \tag{A15}$$

From the above equation we notice that for $l=0$ we get $\frac{\partial^2 q_{00}}{\partial t^2} = 0$ and thus $q_{00}(t) = 0$ (as $q(0) = 0$ and $\lim_{t \rightarrow \infty} q(t) < \infty$). For $l \geq 1$ we get

$$\frac{\partial^2 q_{lm}(t)}{\partial t^2} = -\frac{\omega_p^2 l}{2l+1} q_{lm}(t) + \sum_i \omega_p^2 \frac{l+1}{2l+1} A_{lmi} n \int_0^a \frac{r_1^{l+2} dr_1}{a^{l+2}} j_l(k_{li} r_1) \sin(\omega_{li} t), \tag{A16}$$

which requires the solution form,

$$\begin{aligned}
q_{lm}(t) & = B_{lm}/a^2 \sin(\omega_p \sqrt{\frac{l}{2l+1}} t) \\
& + \sum_i A_{lmi} \frac{(l+1)\omega_p^2}{\omega_p^2 - (2l+1)\omega_{li}^2} n \int_0^a \frac{r_1^{l+2} dr_1}{a^{l+2}} j_l(k_{li} r_1) \sin(\omega_{li} t),
\end{aligned} \tag{A17}$$

and $\delta\rho_2(\mathbf{r}, t) = \sum_{l=1}^\infty \sum_{m=-l}^l q_{lm}(t) Y_{lm}(\Omega) \delta(a-r)$. The first term in Eq. (A17) describes the self-oscillations of surface plasmons, whereas the second one displays the surface plasmon oscillations induced by the volume plasmons. This

induced part of surface oscillations is nonzero only when the volume modes are excited and their amplitudes, A_{lmi} , are nonzero. The frequencies of self-oscillations of the surface plasmons are equal to $\omega_{l0} = \omega_p \sqrt{\frac{l}{2l+1}}$, corresponding to various multipole modes (numbered with l). Note that these frequencies are lower than the bulk plasmon frequency ($\omega_p = \sqrt{\frac{nq^2 4\pi}{m}}$ in Gauss units or $\sqrt{\frac{nq^2}{\epsilon_0 m}}$ in SI), whereas the volume plasmon modes oscillate with frequencies higher than ω_p . Worth noting is also an absence of the temperature dependence of the surface ionic plasmon resonances in contrary to the volume plasmon self-frequencies.

-
- [1] K. Okamoto, I. Niki, A. Scherer, Y. Narukawa, and Y. Kawakami, "Surface plasmon enhanced spontaneous emission rate of InGaN/ GaN quantum wells probed by time-resolved photoluminescence spectroscopy," *Appl. Phys. Lett.* **87**, p. 071102, 2005.
- [2] S. Pillai, K. R. Catchpole, T. Trupke, G. Zhang, J. Zhao, and G. M.A., "Enhanced emission from Si-based light-emitting diodes using surface plasmons," *Appl. Phys. Lett.* **88**, p. 161102, 2006.
- [3] D. M. Schaadt, B. Feng, and E. T. Yu, "Enhanced semiconductor optical absorption via surface plasmon excitation in metal nanoparticles," *Appl. Phys. Lett.* **86**, p. 063106, 2005.
- [4] S. P. Sundararajan, N. K. Grandy, N. Mirin, and N. J. Halas, "Nanoparticle-induced enhancement and suppression of photocurrent in a silicon photodiode," *Nano Lett.* **8**, p. 624, 2008.
- [5] M. Westphalen, U. Kreibig, J. Rostalski, H. Lüth, and D. Meissner, "Metal cluster enhanced organic solar cells," *Sol. Energy Mater. Sol. Cells* **61**, p. 97, 2000.
- [6] A. J. Morfa, K. L. Rowlen, T. H. Reilly, M. J. Romero, and J. Lagemaat, "Plasmon-enhanced solar energy conversion in organic bulk heterojunction photovoltaics," *Appl. Phys. Lett.* **92**, p. 013504, 2008.
- [7] W. Jacak, J. Krasnyj, J. Jacak, R. Gonczarek, A. Chepok, L. Jacak, D. Hu, and D. Schaadt, "Radius dependent shift in surface plasmon frequency in large metallic nanospheres: Theory and experiment," *J. Appl. Phys.* **107**, p. 124317, 2010.
- [8] S. A. Maier, P. G. Kik, and H. A. Atwater, "Optical pulse propagation in metal nanoparticle chain waveguides," *Phys. Rev. B* **67**, p. 205402, 2003.
- [9] P. A. Huidobro, M. L. Nesterov, L. Martin-Moreno, and F. J. Garcia-Vidal, "Transformation optics for plasmonics," *Nano Lett.* **10**, pp. 1985–1990, 2010.
- [10] S. A. Maier, *Plasmonics: Fundamentals and Applications*, Springer, Berlin, 2007.
- [11] A. V. Zayats, I. I. Smolyaninov, and A. A. Maradudin, "Nano-optics of surface plasmon polaritons," *Phys. Rep.* **408**, p. 131, 2005.
- [12] F. J. G. de Abajo, "Optical excitations in electron microscopy," *Rev. Mod. Phys.* **82**, p. 209, 2010.
- [13] W. L. Barnes, A. Dereux, and T. W. Ebbesen, "Surface plasmon subwavelength optics," *Nature* **424**, p. 824, 2003.
- [14] J. M. Pitarke, V. M. Silkin, E. V. Chulkov, and P. M. Echenique, "Theory of surface plasmons and surface-plasmon polaritons," *Reports on Progress in Physics* **70**, pp. 1–87, 2007.
- [15] P. Berini, "Long-range surface plasmon polaritons," *Advances in Optics and Photonics* **1**, pp. 484–588, 2009.
- [16] L. D. Landau and E. M. Lifshitz, *Field Theory*, Nauka, Moscow, 1973.
- [17] J. D. Jackson, *Classical Electrodynamics*, John Wiley and Sons Inc., New York, 1998.
- [18] W. Jacak, "Propagation of collective surface plasmons in 1D periodic ionic structure," submitted.
- [19] J. Jacak, J. Krasnyj, W. Jacak, R. Gonczarek, A. Chepok, and L. Jacak, "Surface and volume plasmons in metallic nanospheres in semiclassical RPA-type approach; near-field coupling of surface plasmons with semiconductor substrate," *Phys. Rev. B* **82**, p. 035418, 2010.
- [20] D. Pines, *Elementary Excitations in Solids*, ABP Perseus Books, Massachusetts, 1999.
- [21] D. Bohm and D. Pines, "A collective description of electron interactions: III. coulomb interactions in a degenerate electron gas," *Phys. Rev.* **92**, p. 609, 1953.
- [22] M. Brack, "The physics of simple metal clusters: self-consistent jellium model and semiclassical approaches," *Rev. of Mod. Phys.* **65**, p. 667, 1993.
- [23] W. Ekardt, "Size-dependent photoabsorption and photoemission of small metal particles," *Phys. Rev. B* **31**, p. 6360, 1985.
- [24] G. Mie, "Beitrige zur Optik trüber Medien, speziell kolloidaler Metallösungen," *Ann. Phys.* **25**, p. 376, 1908.
- [25] M. L. Brongersma, J. W. Hartman, and H. A. Atwater, "Electromagnetic energy transfer and switching in nanoparticle chain arrays below the diffraction limit," *Phys. Rev. B* **62**, p. R16356, 2000.
- [26] I. S. Gradshteyn and I. M. Ryzhik, *Table of Integrals Series and Products*, Academic Press, Inc., Boston, 1994.